International Journal for Housing Science and Its Applications
Publish August 3, 2025. Volume 46, Issue 3 Pages 124-138

https://doi.org/10.70517/ijhsa46309

Big data and AI-driven research on real-time monitoring and fault early warning of bridge structures using integrated learning algorithms

Ruohan Zhang[1,*]
[1] CCCC First Public Bureau Group Co., Ltd., Beijing, 100000, China
Corresponding authors: (e-mail: tjzhenxian@163.com).

Abstract In this paper, sensor data are collected by group wise perception for preprocessing and fusion, SSA method is introduced to divide the output of LSTM into temperature loading effect with periodic trend, and residual data as vehicle loading effect and noise, combined with BDLM method to reduce the noise, increase the accuracy and stability of the model, and effectively monitor the bridge structure in real time. Then the Stacking integrated learning algorithm is used to mix different kinds of base learners to reduce the variance, which effectively improves the generalization ability of the model and realizes the fault warning of the bridge structure. The results show that the proposed method can effectively reduce noise, increase the accuracy and stability of the model, and alleviate the risk of overfitting. The LSTM-SSA-BDLM model can obtain vehicle-induced strain data under lossy and non-destructive conditions, and the four damage assessment indexes of "k, R^2, b and Ta" are stably distributed in the range of 0.45~1.55, which can effectively identify the hypothetical bridge damage. The baseline value of the warning threshold is pre-tested and estimated using the Pareto distribution model, and the value of the mid-span disturbance for a suspension bridge with 95% guarantee is obtained as -0.7076m, which ensures that the baseline value of the threshold can meet the standard of material strength.

Index Terms LSTM, SSA method, BDLM method, Stacking integrated learning, bridge structure monitoring, failure warning

I. Introduction

The construction of highways, railroads and other transportation projects, as an important part of the national infrastructure, has also made leapfrog development, making travel faster and more convenient. Due to China's vast territory and complex terrain, bridge engineering construction is very important in the process of China's transportation network construction. The progress of science, economic development and the continuous maturity of relevant design research theories have contributed to the vigorous development of bridge engineering in China, and the number of bridges put into operation has grown rapidly in recent years [1]-[3]. Bridge facilities play an important role in social development, especially the development of large-span bridges, which largely improves the timeliness and convenience of traffic transportation [4]. Bridges in the later stage of operation and maintenance, with the increasing service life of bridges, will inevitably encounter some problems. At present, there is a considerable part of the bridge service life in more than ten years some, some even reached more than thirty years, although these bridges are designed to serve far more than two or three decades, but part of the bridge in service due to the long-term environment, load, natural environment, the role of the vehicle and so on many aspects of the impact of the bridge, resulting in corrosion aging of the building materials, the accumulation of structural damage to the key parts, and in serious cases lead to the collapse [5]-[8]. At the same time, along with the rapid development of the economy, some bridges designed and built in the last century are difficult to adapt to the current traffic volume needs, traffic flow are far more than the design value, these factors have accelerated the bridge structural damage, the bridge is also a challenge to the long-term safe operation [9]. Some of them even lead to major traffic accidents during the service period of bridges due to poor management by relevant departments, and the transportation department pays more and more attention to the safe operation of bridges. With the continuous emergence of these problems, the bearing capacity of bridges will be affected firstly, the safety coefficient of bridges will be reduced, the safety will be weakened, and the bridges may not be able to reach the design service life, which will pose a threat to people's life safety [10], [11]. By monitoring bridges, timely maintenance and management of bridges can be carried out, while reducing the occurrence of accidents. However, the current inspection of bridges is still carried out periodically, which is difficult to cope with bridge failures caused by sudden damage and accumulated damage.

Therefore, real-time monitoring of bridges and early warning of bridge failures are needed. With various monitoring technologies and early warning methods, bridge management has entered into intelligence. Among them, the drive of big data and artificial intelligence (AI) accelerates the speed and accuracy of data collection and data calculation, and various types of integrated learning algorithms are characterized by accurate predictive performance, which provides a guarantee for bridge operation and maintenance [12], [13].

The assistance of sensors is indispensable in performing real-time monitoring of bridges, but the sensors used and the focus varies from one institute to another. Comisu et al [14] combined visual inspection, multi-sensors and augmented reality deterioration modeling to construct a permanent inspection system that can monitor multiple forms of damage and structural safety parameters of bridges as well as predict the evolution of deterioration mechanisms while reducing the cost of operation and maintenance. VH and Shubhangi [15] created a real-time bridge monitoring method based on wireless IoT technology, consisting of communication devices, four types of sensing devices, and database storage devices. Lin and Chang [16] developed a real-time monitoring system for bridge scour in order to clarify whether the bridge failure under water scour is affected by vibration frequency or rigid body motion, and the monitored data were used to construct a bridge safety evaluation index, which provides a reference for bridge safety warning. Qowiy et al [17] provided an online real-time monitoring system for railroad bridge structures consisting of four types of strain gauges, accelerometers, linear variable displacement and proximity wireless intelligent sensors to form an online real-time monitoring system for railroad bridge structures. Xu and Qiu [18] established a centralized remote real-time bridge health condition monitoring system by using a wireless sensor network and an embedded wavelet neural network for collecting and denoising the vessel data in the monitoring range of a long-span bridge, respectively, with the support of Internet-based technology. Zhang et al [19] designed a dynamic monitoring system for bridge structures, which captured bridge response data in real time through sensors and integrated cloud computing and edge computing to compute the data efficiently. Zeng et al [20] applied strain sensors to acquire bridge data in real time and combined with a modal coordinate transformation method to transform the data into strain and displacement, and performed real-time structural deformation monitoring. Li et al [21] used back propagation neural network and long and short term memory network to learn and analyze the long term real time monitoring bridge data based on the on-site structural health monitoring system in order to predict the response of the bridge under the complex environment. Kokane and Jadhav [22] emphasized on the deflection identification by means of four kinds of sensors, namely, deflection, infrared, water level and vibration, which are four types of sensors for real-time monitoring of bridge structural data, introducing IoT control technology for real-time monitoring of bridge structure and safety, and setting relevant structural thresholds to activate an alarm program when the bridge risk exceeds the thresholds. However, due to the differences in factors such as strain and vibration, the impact of data noise interference is significant, making it difficult to guarantee the accuracy of these monitoring methods.

In terms of early warning for bridges, Riyansyah et al [23] proposed a bridge condition assessment and early warning system for wireless sensor network monitoring, which performed acceleration-frequency transformation, displacement and effective stiffness confirmation of the monitored data, and simulated different levels of bridge damages combined with a finite element model to determine the location of bridge damages. Jiang et al [24] integrated small wave packet analysis and fuzzy comprehensive evaluation to analyze and judge the damage condition of the bridge, and combined with mathematical statistical analysis and principal component analysis to provide early warning of structural damage of the bridge on the basis of assessment. Zhu et al [25] used Gaussian process model to select the bridge performance data and capture the relevant uncertainty between the data to achieve the health state assessment and abnormal warning of the bridge. Wang et al [26] brought together partial least squares analysis, Euclidean distance similarity measure, local linear regression model, and principal component analysis to develop a methodology that can realize the abnormal frequency warning of bridges with different environmental conditions. Li et al [27] predicted and clustered the error values and predicted values of bridge response data by using long and short-term memory network and expectation maximization-Gaussian hybrid model to accomplish the bridge under the influence of uncertain environmental factors Dynamic Early Warning.

In this paper, data from the bridge system is collected using swarm intelligence sensing and transmitted by wired or wireless means. Multi-sensor fusion using D-S evidence theory algorithm is used to realize the overall structural data of the bridge. After that, the Long Short-Term Memory Network (LSTM) method is used to output the temperature loading effect with periodic trend through Singular Spectrum Analysis (SSA), and the residual data as vehicle loading effect with noise. Meanwhile, the BDLM method is used to dynamically correct the decomposed vehicle load effect and noise, and finally the LSTM-SSA-BDLM prediction framework is established as a way to accurately estimate the expected behavior of the bridge structure. Then the Stacking method in integrated learning is used to improve the generalization ability of the model by reducing the model prediction variance, so as to avoid the lower limit problem brought by a single deep model and further improve the model's early warning confidence,

and this model is used to assess and warn the damage state of the bridge, as well as determining the dynamic threshold of safety warning for the bridge structure.

II. Stacking algorithm-based bridge structure monitoring and failure warning model

II. A. Data Processing of Bridge Intelligent Early Warning System

II. A. 1) Data perception

Bridge monitoring sensors focus on key areas in conjunction with the characteristics of the specific bridge, its environment, and the requirements of the safety assessment during the operational phase. This paper proposes a combination of fixed sensors and swarm sensing sensors to monitor bridge equipment. The monitoring programs in this paper are mainly divided into: stress, environment, displacement and tilt monitoring. Among them, stress monitoring is used to monitor the main girder pressure, vibration acceleration and cable pressure, which is placed on the main arch, ground and boom; displacement monitoring is used to monitor the longitudinal slip of the bridge deck and the deflection of the arch ribs, which is placed at the arch foot and the arch rib mid-span; tilt monitoring is used to monitor the inclination of the bridge, which is placed at the arch foot; and environment monitoring is used to monitor seasonal and insolation-induced temperature changes, which is placed at the main arch ribs and the ground.

II. A. 2) Data transmission

Data transmission ensures that a stable physical connection is established between the various components of the monitoring system to ensure that monitoring data and commands are transmitted safely, reliably and with high quality within the system. The long-distance data transmission between the on-site monitoring unit and the data center adopts fiber optic transmission technology, wireless transmission technology and a combination of the two, and wireless networks such as NB-IoT and 5G are adopted for bridge areas with inconvenient traffic, complex terrain and difficult physical wiring.

II. A. 3) Data pre-processing

This system uses data cleaning methods to process sensor data in the order of missing values, outliers, and duplicate values processing. Firstly, multiple linear regression interpolation is used to fill the missing values. For the bridge system at the same moment, if the overall structure of the bridge is abnormal, some of the sensor data will change accordingly, so the data from different sensors have correlation, and this method is to use the correlation of the data to establish a regression equation to fill the missing values.

This system uses the nearest neighbor sorting algorithm to screen and remove duplicate values from the dataset. First of all, based on the type of sensor, the data set is disaggregated and arranged, and the selected class of sensor data is arranged in ascending order, so that similar or the same monitoring data are adjacent to each other; then a sliding window of size w is set up for the sorted sensor data, and each time the data in each row of the sliding window is screened for similarity in terms of the Euclidean distance. The first row of data in the window is compared with the remaining $w-1$ rows of data, and if it meets the judgment criterion of Euclidean distance, this row of data is deleted, and other data are processed in turn. After data cleaning, data that meets the quality can be obtained and input to the fusion system.

II. A. 4) Data fusion

Data fusion fuses multiple heterogeneous sensors in the following steps: Firstly, the basic probability distribution function of the sensor is constructed according to the warning threshold, and the construction method based on the sample value is used here. Secondly, the D-S evidence theory algorithm is used for data fusion to obtain the fused warning level and realize the warning function. On the basis of the original algorithm, a genetic algorithm is used to weight the optimization and improve the credibility of the warning.

II. B. SSA-LSTM-BDLM prediction framework design

II. B. 1) LSTM networks

LSTM [28] is a type of recurrent neural network (RNN) whose structure consists of three gates: an input gate, a forgetting gate and an output gate. The equations of LSTM are as follows:

(1) The forgetting gate f_t determines how much previous information should be retained by the model in the current time step, i.e.:

$$f_t = \sigma(W_f o[h_{t-1}, x_t] + b_f) \tag{1}$$

where: $\sigma(\cdot)$ expresses the Sigmoid function; x_t denotes the current input. h_{t-1} is the hidden state, which is linearly transformed using the weights W_f and the bias term b_f.

(2) The input gate i_t controls how much new information $\tilde{c}_t$ is stored by the LSTM network into the current cell state c_t, i.e.:

$$i_t = \sigma(W_t[h_{i-1}, x_t] + b_t) \tag{2}$$

(3) Candidate memories $\tilde{c}$ that create a new information vector by applying a hyperbolic tangent (tanh) activation function:

$$\tilde{c}_t = \tanh(W_c[h_{t-1}, x_t] + b_c) \tag{3}$$

The above equation is similar to the forgetting gate, but the weights and bias terms (W_t and b_t) are different, and the subscript c denotes the corresponding cellular state, i.e., the state of the information storing the long-term memory in the LSTM network.

(4) Memory cell:

$$c_t = f_t c_{t-1} + i_t \tilde{c}_t \tag{4}$$

(5) Output gate:

$$o_t = \sigma(W_o[h_{t-1}, x_t] + b_o) \tag{5}$$

where W_o and b_o are the weight and bias terms, respectively.

(6) The hidden state h_t is the output of the LSTM, which is generated by the weighted product of the cell state c_t and the output gate o_t:

$$h_t = o_t \tanh(c_t) \tag{6}$$

The LSTM parameters in this paper are set as follows: the maximum number of training rounds in the training set is 200 using the Adam optimizer, each small batch contains 10 samples, the initial learning rate is 0.005, the learning rate is reduced every 100 iteration cycles, and the percentage of learning rate reduction is set to 0.1.

II. B. 2) Singular spectrum analysis methods

Singular Spectrum Analysis (SSA) [29] aims to decompose the original sequence into a small number of sums of independent interpretable components. In this paper, we mainly combine the SSA method to extract the long-term trend and periodic terms in the extreme deflection series, and the method steps are as follows:

(1) Choose a suitable window length L to lag the original sequence $\{x_1, x_2, \cdots, x_n\}$ to obtain the trajectory matrix as follows:

$$X = \begin{Bmatrix} x_1 & x_2 & \cdots & x_{n-L+1} \\ x_2 & x_3 & \cdots & x_{n-L+2} \\ \vdots & \vdots & & \vdots \\ x_L & x_{L+1} & \cdots & x_N \end{Bmatrix} \tag{7}$$

where: n is the length of the sequence and L takes the cycle length of the sequence.

(2) Singular value decomposition (SVD) of the trajectory matrix.SVD will decompose the trajectory matrix into three matrices: an orthogonal matrix U, a diagonal matrix S and another orthogonal matrix V:

$$X = USV^{\text{ú}} \tag{8}$$

(3) Principal component grouping: By grouping the corresponding columns in U, S and V, the principal components of the time series can be obtained. These principal components can represent different characteristics of the time series, such as trend, periodicity and noise, etc. for the i th principal component:

$$T_t = s_t u_t v_t^{\cdot} \tag{9}$$

where s_t is the element on the diagonal of the diagonal matrix S, called the singular value, which represents the energy magnitude of each component of the time series. u_t and v_t are the column vectors of U and V, which denote the left singular vector and the right singular vector, respectively.

(4) Sequence reconstruction: the selected principal components are inverted to obtain the reconstructed sequence. For the selected principal components in this paper the reconstructed sequence is as follows:

$$X_2 = T_1 + T_2 \tag{10}$$

Diagonal averaging is then performed to convert back to the original sequence format.

II. B. 3) BDLM method considering error updating

BDLM is a dynamic linear model based on Bayesian statistical methods.The dynamic part of the BDLM model consists of a linear state-space model for describing the state of the system over time. The core idea of the BDLM method for error parameter updating is to use the t distribution to approximate the overall error distribution, defined as follows.

Monitoring Equation:

$$y_t = \theta_t + v_t, v_t \sim N(0, V) \tag{11}$$

Combined with the physical a priori knowledge that the vehicle loading effect and noise etc. have a linear trend during the monitoring time, in order to estimate the true state information after noise elimination, the state equation can be written as:

$$\theta_t = G_t \theta_{i-1} + w_t, w_t \sim N(0, W_t) \tag{12}$$

Initial information:

$$(\theta_0 \mid D_0, \varphi) \sim N(m_0, V_t C_0) \tag{13}$$

$$(\varphi \mid D_0) \sim \Gamma[n_0 / 2, d_0 / 2] \tag{14}$$

where: y_t and θ_t are observation and state values, respectively; v_t and w_t are independent and mutually independent monitoring and state errors; $G_t = 1$ is the state transfer coefficient; V_t is the unknown variance of the monitoring error, W_t is the state error variance; $N(\cdot)$ is the normal probability density function; $\Gamma(\cdot)$ is the chi-square distribution probability density function; and $\varphi^{-1} = V_t^{-1}$.

The detailed probabilistic recursion method is as follows:

(1) $t-1$ moment of the posterior distribution:

$$(\theta_{t-1} \mid D_{t-1}) \sim T(m_{t-1}, C_{t-1}) \tag{15}$$

$$(\phi_{t-1} \mid D_{t-1}) \sim \Gamma(\frac{n_{t-1}}{2}, \frac{d_{t-1}}{2}) \tag{16}$$

(2) The prior distribution of the t moment:

$$(\theta_t \mid D_{t-1}) \sim T(m_t, C_t) \tag{17}$$

$$(y_t \mid D_{t-1}) \sim T_{s_t}(f_t, Q_t) \tag{18}$$

(3) The posterior distribution at moment t:

$$(\theta_i \mid D_i) \sim T(m_i, C_i) \tag{19}$$

Its recursive relationship:

$$\begin{aligned} m_t &= G_t m_{t-1} + A_t e_t \\ C_t &= (S_i / S_{i-1})[R_i - A_i A_i' Q_i] \\ n_i &= n_{i-1} + 1 \\ d_i &= d_{i-1} + S_{t-1} e_t^2 / Q_t \\ S_t &= d_i / n_t \\ e_t &= y_t - f A_t = R_i / Q_t \end{aligned} \tag{20}$$

The initial value of the noise distribution parameter V_t is replaced by the estimate S_{t-1}.

II. B. 4) LSTM-SSA-BDLM approach

The LSTM-SSA-BDLM state space equations established in this paper are as follows:

$$\tilde{Z}_t = G(Z_{t-1}) = X_t + Y_t + v_t + u_t, v_t \sim N(0,V), u_t \sim N(0,U) \tag{21}$$

$$X_t = X_{t-1} + w_t, w_t \sim N(0,W_t) \tag{22}$$

Where $G(\cdot)$ denotes the LSTM prediction function, the input Z_{t-1} is the sensor monitoring data at the moment $t-1$, and $\tilde{Z}_t$ is the predicted value updated based on the LSTM network at the moment t, which can be regarded as the expectation of the prediction distribution due to the existence of prediction error. X_t denotes the vehicle loading effect, and Y_t is the long-term trend and periodic trend data obtained from SSA decomposition. v_t is the vehicle loading noise, and u_t is the random fluctuation of long-term trend and periodic trend obtained by SSA method decomposition. Where u_t is small enough to be negligible.

The forecasting accuracy of the model can be measured by the Root Mean Square Error (RMSE), which is very sensitive to the reflection of extra-large or extra-small errors in a set of measurements, and thus can be a good reflection of the forecasting accuracy, calculated as follows:

$$RMSE = \sqrt{\frac{\sum_{t=1}^{n} (y_t - \tilde{y}_t)^2}{n}} \tag{23}$$

where: y_t and $\tilde{y}_t$ are the monitored and predicted values, respectively; n is the number of predicted samples.

II. C.Prediction integration strategies and dynamic warning interval setting methods

II. C. 1) Optimization algorithm based on integrated learning

The integration learning method is applicable to deep learning models, which can further improve the generalization performance of the models. Based on this, this paper adopts the integration learning method to integrate the prediction model in order to improve the generalization ability of the response prediction model.

(1) Model generalization ability measurement index

In statistical learning, it is common to use bias and variance to measure the generalization ability of a model. Where the bias $Bias[\hat{f}]$ is the mean of the prediction error and represents the statistical shift of f between the model $\hat{f}$ obtained from training and the ideal model. The variance $Var[\hat{f}]$ is the variance of the prediction value, which indicates the size of the difference between the models obtained from each learning.

(a) Mathematical definition of generalization error

For the sample set $D = \{(x_1, y_1), \ldots, (x_n, y_n)\}$, where the input features $\forall x \in \{x_1, \ldots, x_n\}$, and their corresponding labels $\forall y \in \{y_1, ..., y_n\}$. There exists an ideal optimal model f such that $y = f(x) + \varepsilon$. where ε is unlearnable independent noise. Thus the model $\hat{f}$ is made as close as possible to the ideal model f by learning the model $\hat{f}$ in the sample set D during the training phase of machine learning. The bias-variance decomposition formula for the MSE decomposition of the model on the data set D is:

$$\begin{aligned} E[(y - \hat{f}(x))^2] &= E[((f - E[\hat{f}]) + \varepsilon - (\hat{f} - E[\hat{f}]))^2] \\ &= (f - E[\hat{f}])^2 + E[\varepsilon^2] + E[(\hat{f} - E[\hat{f}])^2] \end{aligned} \tag{24}$$

Also since the expectation of the true value $E[f]=f$, the expectation of the noise ε $E[\varepsilon]=0$, and the variance of the noise is denoted as $Var[\varepsilon]=\sigma^2$, the MSE of the model on the test set can be specifically expressed as the bias $Bias[\hat{f}]$, variance $Var[\hat{f}]$, and data collection error σ^2 composed as:

$$E[(y-\hat{f}(x))^2]=Bias[\hat{f}]^2+Var[\hat{f}]+\sigma^2 \tag{25}$$

(b) Generalization error reduction methods

The generalization error of the model can be reduced by way of reducing the above three errors, and in practical engineering, the σ^2 can be effectively reduced by improving the quality of data collection and reducing the noise of the data itself. The bias $Bias[\hat{f}]$ can be reduced by the way of increasing the complexity of the neural network model or the way of Boosting in integrated learning.

(2) Introduction to the Integration Algorithm

Bagging is a method of combining multiple unstable models to obtain a relatively stable model. Bagging requires firstly to train n homogeneous base models independently and in parallel at the same time, and after the models have been trained, the outputs of the base models are averaged together to obtain the final result.

Boosting is a method that combines multiple weak models with high bias to obtain an integrated model with low bias.The Boosting method first trains n weak models sequentially, and then the latter model is retrained again using the output of the previous model as input, so that the model focuses on samples that have a high prediction error of the previous model.

The Stacking algorithm reduces variance by mixing different kinds of base learners. It can directly train the base model using the same dataset, reducing the variance of the predicted values of the regression task through the variety of model types.

II. C. 2) Stacking-based weight estimation algorithm

The base model learning algorithm is denoted as algorithm $\xi_1,...,\xi_K$, and the metamodel learning is denoted as algorithm ξ. For the i th structural response prediction result output based on the learning algorithm at moment T is denoted as $\xi_t(X_T)=\hat{y}_{T,i}$, where $i=\{1,...,K\}$. Notate $\hat{y}_T$, simplifying as $\hat{y}_i=[\hat{y}_i^1,...,\hat{y}_i^F]^T$, where F is the number of variables of the multivariate prediction task, i.e., the number of sensors to be predicted. The outputs of the K base models are spliced as $Y^{oc}=(\hat{y}_1,...,\hat{y}_K)$.

(1) Breiman's method

Breiman proposes the generalized linear model and the Stacking method [30] combined with an integration strategy that assigns weights to each base model based on its performance on the historical craniometry task. The Breiman method is formulated as follows:

$$\xi(X)=\sum_{i=1}^{K}\theta_i\hat{y}_t \tag{26}$$

where the scalar $\hat{y}_i$ is the prediction of the i th base model and θ_i is the corresponding weight. For $i\in\{1,...,k\}$, the weights assigned to each model need to satisfy the following conditions:

$$\sum_{i=1}^{k}\theta_i=1,\theta_i\geq 0 \tag{27}$$

The weights θ_i contributed by the base model should be non-negative and the sum of the weights θ_i is 1.

In the multivariate task prediction integration task, there is a need to extend the method for Breiman, which targets the model $\hat{y}_i$ with a scalar output, to an integration method for vectors $\hat{y}_i$:

$$\xi(X)=\sum_{i=1}^{K}\theta_i\hat{y}_i \tag{28}$$

For the multivariate prediction of the task of the need to consider the contribution of each target by each model, and then the allocation of weights, this paper multivariate $\hat{y}$ prediction of the task of integration of the formula for:

$$\hat{y}=\xi(X)=\sum_{i=1}^{K}\theta_i\hat{y}_i \tag{29}$$

where, for $\forall i \in \{1,...,K\}$, θ_i is the weight matrix of the multivariate vector $\hat{y}_i$ for the output of the i th base model:

$$\theta_i = \begin{pmatrix} \theta_i^1 & & \\ & \ddots & \\ & & \theta_i^F \end{pmatrix} \tag{30}$$

For $j = \{1,...,F\}$, θ_i^j is the weight of the contribution of the model at the i th model on the prediction of each target $\hat{y}_i^j$.

Thus the output of the final integrated model can be written as:

$$\xi(X) = \begin{bmatrix} \sum_{i=1}^{k} \theta_i^1 \hat{y}_i^1 \\ \vdots \\ \sum_{i=1}^{k} \theta_i^F \hat{y}_i^F \end{bmatrix} \tag{31}$$

where the $\xi(X)$ output of the integrated model has a multivariate vector with the j th row corresponding to the integrated output value of the structural response of the j th sensor, obtained by weighting and summing the outputs of each model for that sensor. And the weights θ_i^j need to satisfy the following two conditions:

$$\begin{aligned} &\theta_i^j \geq 0, \forall i \in \{1,...,K\}, \forall j \in \{1,...,F\} \\ &\sum_{i=1}^{K} \theta_i^j = 1, \forall j \in \{1,...,F\} \end{aligned} \tag{32}$$

That is, the weights contributed by each model need to be non-negative and the sum of the contribution weights of each model for each prediction target is 1. The estimation of the optimal weights θ^* under the above constraints is then carried out by least squares on the dataset D:

$$\theta^* = \arg\min_{\theta} \| \xi_D^{\theta}(Y^{oc}) - y \|_2, s.t.(5-8) \tag{33}$$

(2) Dynamically integrated weight estimation

The Breiman method uses historical data for the estimation of individual base model weights, which refers to data collected in the past that may contain a wider range of situations, a larger range of variability, and a larger sample. In order to discuss the implications of long-term weight estimation and short-term weight estimation for the new prediction task, this paper further discusses two methods that consider short-term estimation based on the Breiman method. They are:

(a) LS-E

The weights of the base model are estimated using the historical data D_L and the combined post-data of the neighboring cycles D_s, i.e., the data used for weight estimation is $D = (D_L, D_S)$.

(b) S-E.

Weight estimation of each base model using data from the adjacent previous cycle D_s. The factors affecting the integration effectiveness of the Stacking method include the selection of the base model in addition to the integration strategy. This chapter mainly focuses on the integration algorithm, and the selection aspect of the base model is not emphasized. Since the integration method of Stacking requires the base model to be a strong model with excellent prediction performance, and considering that the integration of a poorly performing model will reduce the accuracy of the integrated model, the LSTM-SSA-BDLM model is chosen as the basis of the integrated model for the study of the Stacking method.

III. Analysis of early warning results of bridge structure monitoring and fault diagnosis

III. A. Anomaly data diagnosis based on bridge structure

III. A. 1) Subject of the study

In this section, the monitoring data of Jiangyin Bridge, a large-span bridge, is used as a research object to demonstrate the feasibility of diagnosing anomalous data based on LSTM-SSA-BDLM.

Jiangyin Bridge, a 1385m main span suspension bridge located in Jiangsu Province, China, was completed in 1999 and became the largest span bridge in China at that time. The main span is a streamlined flat steel box girder with a height of 3 m and a width of 36.9 m. The heights of the south and north towers are 187 m and 184 m. The health monitoring system of the JYB was upgraded in 2005 to include anemometers, Global Positioning System (GPS), fiber optic strain gauges, thermometers, and accelerometers. Five transverse accelerometers and ten vertical accelerometers are arranged along the main girders at 1/8, 1/4, 3/8, 1/2 and 3/4 of the main span, and the sampling frequency of the accelerometers is 50Hz.

III. A. 2) Lateral acceleration during ship collision at Jiangyin Bridge

At about 20:14 on June 2, 2005, a pile driving vessel collided with the main girder of the JYB. Meanwhile, the structural health monitoring system successfully recorded the acceleration response of the bridge. Since the ship collision force is generally along the transverse direction, the transverse acceleration is extremely sensitive to ship impact and is considered in this section. Although the impact location was close to 1/4 of the main span, the accelerometers AD5CL and AD7CL recorded some unknown events simultaneously. Therefore, only the AD9CL accelerometer was selected to verify the validity of the LSTM-SSA-BDLM. The average value was taken for every 50 points to reduce the measurement noise and uncertainty. Figure 1 shows the lateral acceleration during ship impact on Jiangyin Bridge. It can be seen that the lateral acceleration fluctuates significantly around 20:15 when the ship impacts the bridge.

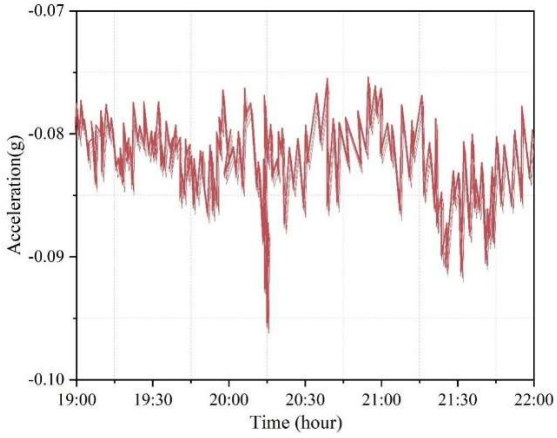

Figure 1: Transverse acceleration during collision of jiangyin bridge

The acceleration has a nonlinear strong dynamic change characteristics, but no obvious periodicity. Therefore, LSTM-SSA-BDLM is established to identify the outliers of acceleration response of Jiangyin Bridge. The form of LSTM-SSA-BDLM is as follows:

$$F_{Ac} = \begin{bmatrix} 1 & 0 & 1 & 0 \end{bmatrix} \tag{34}$$

$$G_{Ac} = \begin{bmatrix} 1 & 1 & 0 & 0 \\ 0 & 1 & 0 & 0 \\ 0 & 0 & \phi_{Ac,1} & \phi_{Ac,2} \\ 0 & 0 & 0 & 0 \end{bmatrix} \tag{35}$$

$$V_{Ac} = \sigma_{Ac}^2 \tag{36}$$

$$W_{Ac} = blockdiag[(\sigma_{Ac}^{\theta})^2 \quad (\sigma_{Ac}^{\beta})^2 \quad (\sigma_{Ac}^{AR})^2 \quad 0] \tag{37}$$

The LSTM-SSA-BDLM parameters to be estimated are:

$$\Theta_{Ac} = \begin{bmatrix} \phi_{Ac,1} & \phi_{Ac,2} & \sigma_{Ac} & \sigma_{Ac}^{\theta} & \sigma_{Ac}^{\beta} & \sigma_{Ac}^{AR} \end{bmatrix} \tag{38}$$

To ensure computational efficiency, the LSTM-SSA-BDLM is built using the acceleration response every 10 minutes, and then the data within the next 10 minutes are diagnosed. Therefore, the LSTM-SSA-BDLM parameters and thresholds are updated every 10 minutes to accommodate different acceleration characteristics. Note that when

consecutive anomalous data are recognized, the updating of the model parameters is stopped until the acceleration within the next 10 minutes is free of outliers. The first 20% of data within each 10-minute period is used to estimate the LSTM-SSA-BDLM parameters and thresholds. For acceleration data within 19:00 to 19:10, the LSTM-SSA-BDLM parameters are:

$$\Theta_{\Lambda c} = \left[0.4177 \quad 0.441 \quad 2.26\times10^{-4} \quad 6.9\times10^{-5} \quad 1.26\times10^{-5} \quad 5.92\times10^{-5}\right] \tag{39}$$

With its threshold value of 9.0516, this paper represents the change in the log-likelihood function between 19:00 and 19:10. Figure 2 shows the threshold and the log-likelihood difference between 19:10 and 22:00 for the neighboring time steps. The algorithm stops when the number of iterations reaches only 27, which is partly due to the fact that there are fewer parameters to be estimated, and partly an indication of the efficiency of the initialization of the subspace method.

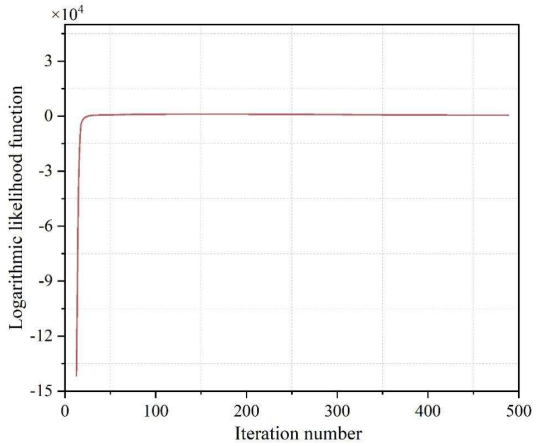

Figure 2: The logarithm of the threshold and the adjacent time step

The variation of the log-likelihood differences is shown in Figure 3. It can be noticed that all log-likelihood differences are smaller than the threshold between 19:10 and 20:14. However, the log-likelihood differences suddenly increase around 20:10:10 and most of the log-likelihood differences are significantly above the threshold between 20:10:10 and 20:15:20. After 20:15:20, the log-likelihood difference drops below the threshold. This duration corresponds to the time of the ship collision, proving the effectiveness of diagnosing the acceleration data based on LSTM-SSA-BDLM. Based on the above analysis results, it can be known that the outliers caused by the ship collision lasted for nearly 5 minutes. Based on the estimated LSTM-SSA-BDLM parameters, further predictions can be made using Bayesian inference.

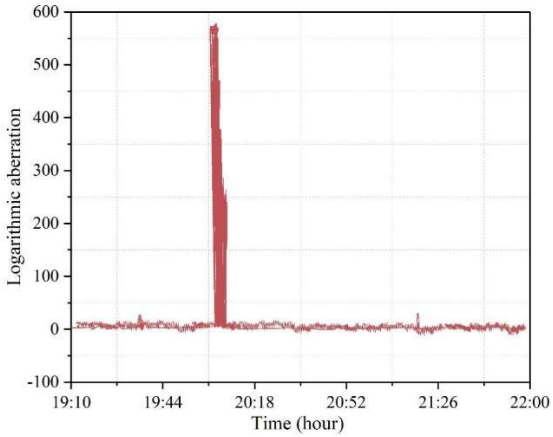

Figure 3: Logarithmic variation

The results of the forward step prediction based on LSTM-SSA-BDLM are shown in Fig. 4. Fundamentally, data reconstruction by LSTM-SSA-BDLM belongs to the prediction problem, i.e., the prediction results are utilized to

replace the anomalous data. Since LSTM-SSA-BDLM only performs well in finite step forward prediction, it is not accurate in diagnosing continuous outliers. In addition, acceleration change is a typical nonlinear stochastic dynamic process, and the predicted values are not substituted for the detected acceleration anomalies in order to ensure the accuracy of LSTM-SSA-BDLM. The LSTM-SSA-BDLM based method only needs 0.3546s to process 500 acceleration data and estimate the model parameters, so the method detects a single data point consumes an average of 0.0312 s. From the above analyzed results, it can be seen that the anomaly identification method based on the LSTM-SSA-BDLM has a better performance in terms of both accuracy and computational efficiency.

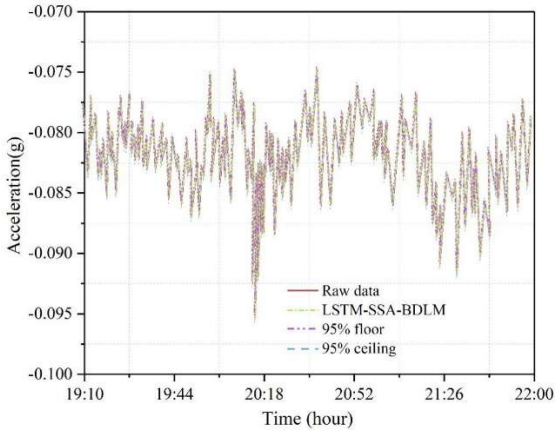

Figure 4: A forward prediction result based on LSTM-SSA-BDLM

III. B. Bridge Damage State Assessment and Early Warning

Damage assessment for the bridge structure as a whole should focus on the performance of multiple measurement points rather than a single measurement point; therefore, the damage assessment metrics averaged over eight measurement points (the mean of the metrics at multiple measurement points) were used for bridge damage assessment. The regression error T_a, the coefficient of the primary term k and the constant term b of the regression equation, and the goodness-of-fit of the scatter points about the regression equation R^2 were used, and due to the difference in the physical significance and order of magnitude of the four indicators of damage assessment of k, R^2, b and T_a, a value of the converted bias C was introduced for the convenience of examination to conduct the unified conversion:

$$C = \frac{A_{mean}}{B_{mean}} \tag{40}$$

where A_{mesm} is the mean value of multi-measurement point index of one test set; B_{mean} is the mean value of all test sets A_{mesm}.

In the selected period of the measured data, it was determined that there was no new damage to the bridge during the period by manual inspection of the bridge, so the measured data were considered to be nondestructive, and thus the measured data of the period could be used as the benchmark for determining whether there was new damage or not. The vehicular strain data of the left span of the main bridge of Siantang Bridge in a certain month were selected and inputted into the measured multi-input correlation model, and the four damage assessment indexes were calculated in a period of 1 h. The data were then analyzed and the damage assessment indexes were calculated in the same period.

III. B. 1) Numerical distribution of damage assessment indicators for measured data

The distribution of the measured data damage assessment index values is shown in Fig. 5, where the solid lines are the upper and lower limits of the distribution, where (a)~(d) represent the conversion errors under the conditions of k, R², b and Ta, respectively. It can be seen that: k conversion deviation is 0.4754~1.5432, R² conversion deviation is 0.9349~1.0785, b conversion deviation is 0.7106~1.4505, and Ta conversion deviation is 0.9537~1.0438, and the four indexes are all stably distributed within a certain range, with less fluctuation, indicating that there is no new damage of the bridge in the near future.

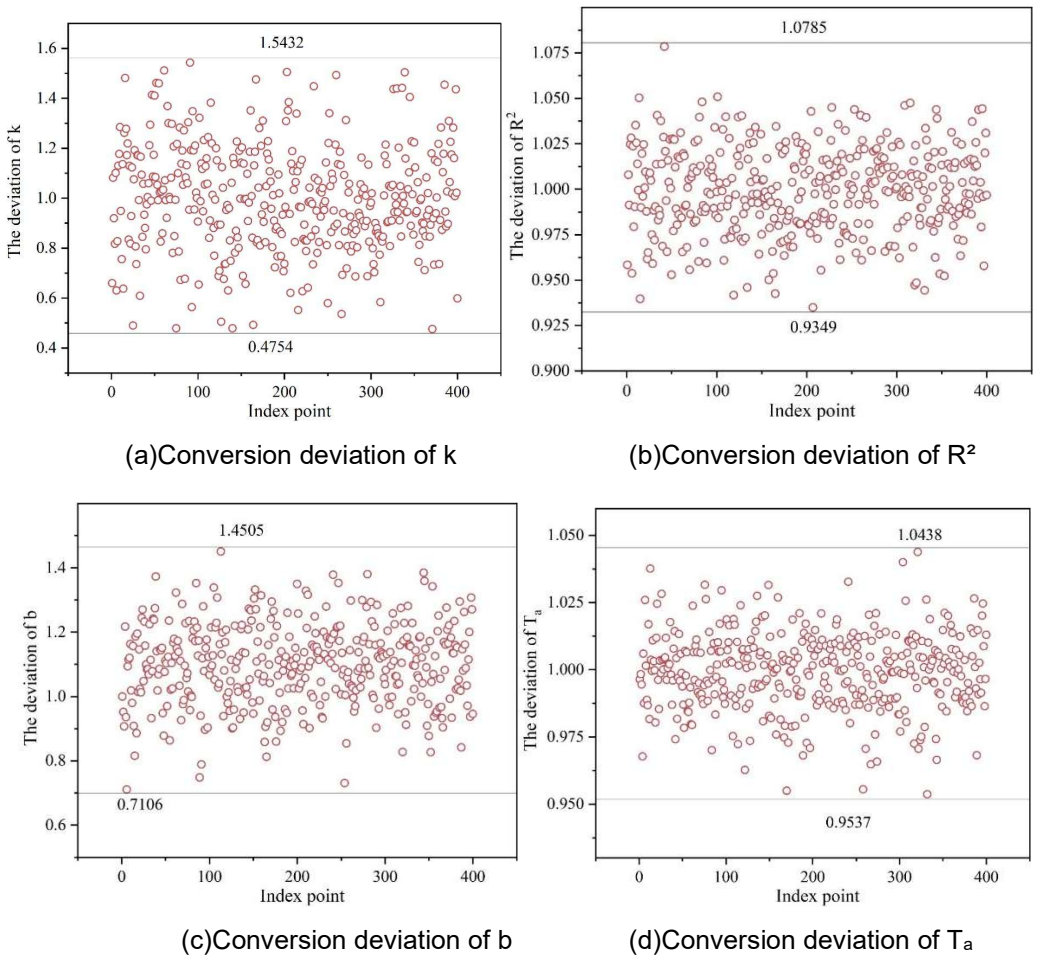

(a)Conversion deviation of k (b)Conversion deviation of R²

(c)Conversion deviation of b (d)Conversion deviation of T_a

Figure 5: Measured data damage assessment index distribution

III. B. 2) Numerical distribution of damage assessment indicators for simulated data

In order to judge the sensitivity of the long-term distribution of the four damage assessment indexes to damage, a certain number of non-destructive and destructive data sets were generated by using the finite element model and input into the simulated multi-input correlation model for the calculation of the four damage assessment indexes. The distribution of the damage assessment indexes in the simulated data is shown in Fig. 6. The values in the figure are the maximum values of the damage assessment indexes on the lossless data set, where (a)~(d) represent the conversion errors under the conditions of k, R ², b and Ta, respectively. From the figure, it can be seen that the thresholds of k, R ², b and Ta are 1.0783, 1.073, 1.4804 and 1.0454, respectively, while more than 90% of the index points in the damaging condition 1 (5% damage) exceed the thresholds of the corresponding indexes, and all the indexes in the damaging condition 2 (10% damage) have already exceeded the thresholds.

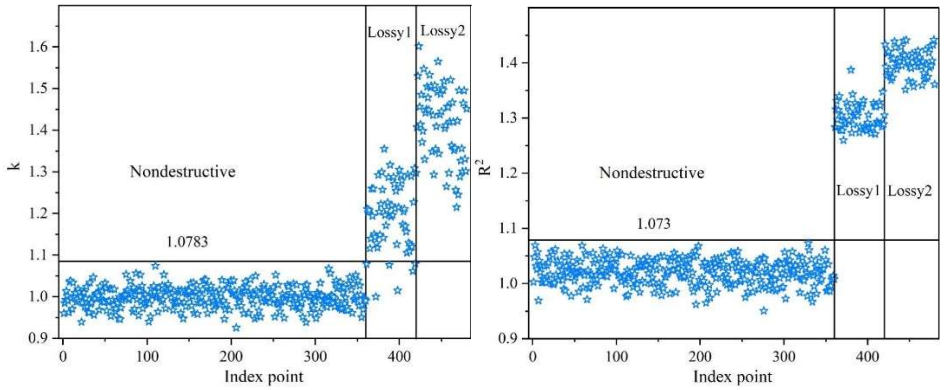

(a)Conversion deviation of k (b)Conversion deviation of R²

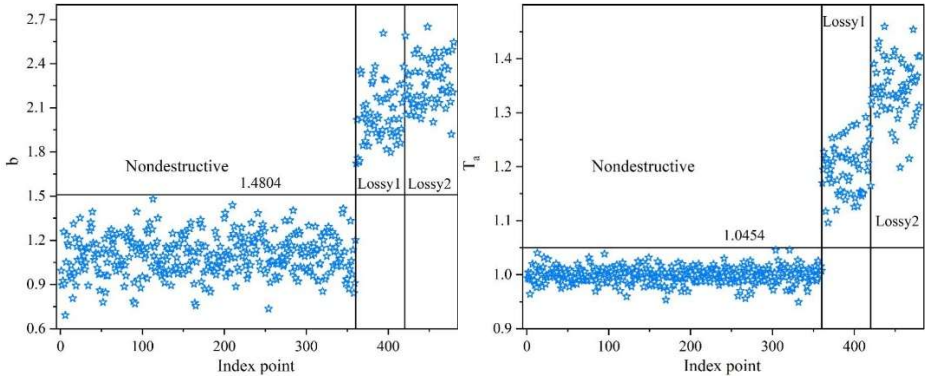

(c)Conversion deviation of b (d)Conversion deviation of T_a

Figure 6: Numerical distribution of simulated data damage assessment index

III. B. 3) Rate of exceedance of injury assessment indicators

The exceedance rates of the four damage assessment indicators in the two damage conditions are shown in Table 1. From the table, it can be seen that there is an exceedance rate of less than 10% in the damage condition 1, which may be due to the relative insensitivity of the corresponding damage assessment indicators to the low percentage of damage, and then it is necessary to combine with the exceedance of other indicators to determine whether it is necessary to issue an early warning. In fact, there is a certain probability that a single indicator will generate false alarms in a certain assessment, therefore, choosing to use four indicators for damage assessment at the same time can analyze whether the data contain damage characteristics from multiple perspectives, thus reducing the probability of false alarms. Therefore, assuming that 75% of the damage assessment indicators exceed the limit at the same time, a warning can be issued.

In summary, it can be seen that in the non-destructive state, each damage assessment index is stably distributed within a certain limit value range. If the bridge structure is damaged during the subsequent monitoring period, the strain correlation between each measurement point changes, and the damage identification and early warning of the bridge structure can be realized by the multi-input model and multi-measurement point damage assessment indexes constructed in this paper.

Table 1: Four damage assessment indicators are under two damage conditions

Loss condition	Overlimit rate(%)				Warning rate(%)
	k	R^2	b	T_a	
1	90	100	100	100	90
2	100	100	100	100	100

III. C. Determination of dynamic thresholds for early warning of structural safety of bridges

In this section, the Pareto distribution model is utilized to pre-test and estimate the baseline value of the warning threshold as a means of ensuring that this threshold baseline value will meet the assurance rate of the material strength criteria, and will also need to be compatible with the baseline service life of the bridge design. By focusing on historical data, the likelihood of such extreme events occurring in a given time domain can be estimated, and the threshold benchmark value can be set accordingly to the value of the correlation index under this probability. In this way, in a new scenario, the system initiates an alert once the metric value of the event that occurs exceeds the threshold baseline value. The specific steps are as follows:

Step 1: Prepare data. Collect relevant historical data, including the variable values of the factors and their corresponding warning situations. Step 2: Establish Pareto distribution model. Based on the collected data, establish a generalized Pareto distribution model.

Specifically, the Pareto distribution model is a probabilistic model suitable for dealing with extreme cases such as tail data and outliers.

Step 3: Set the guarantee rate. According to the engineering needs, set the assurance rate of the threshold base value, aiming to maintain the consistency of the threshold base value with the standard value taken for material strength and the bridge design base period.

Step 4: Obtain the threshold quantile. By modeling the Pareto distribution and setting the base period to be within T years, the x_p estimate of the quantile can be expressed as:

$$x_p = u_0 + \frac{\hat{\sigma}}{\hat{\xi}}[(\frac{n}{N_u}(1-p))^{-\hat{\xi}} - 1] \tag{41}$$

where the solution p of $(1-p)^T = 1 - Pr$ is the quantile corresponding to the credibility of the early warning indicator; $\hat{\xi}$ is the estimate of the shape parameter; $\hat{\sigma}$ is the estimate of the scale parameter; n is the number of samples; and N_u is the number of samples exceeding the threshold.

Step 5: Setting the warning threshold benchmark value Set the quartile obtained in step 4 as the warning threshold benchmark value. The system will issue a warning signal when the observed indicator value exceeds this threshold datum value in a new situation.

This threshold is reached when the state of the bridge really reaches a dangerous level. Therefore a mild warning threshold needs to be established. The mid-span deflection of the bridge is used as the warning benchmark to verify the feasibility of determining the dynamic anomaly warning threshold proposed above. It is known that the sampling frequency of the sensor is 25Hz and the accuracy of the dynamic measurement in the vertical direction is 32mm2ppm. The determination of dynamic thresholds is investigated based on the mid-span disturbance data of this suspension bridge.

Figure 7 shows the four-month mid-span disturbance data for the study bridge for the year 2024. After the predicted data is processed for temperature effect separation and noise reduction, Pareto polar analysis is utilized to predict the base value of the threshold. In this section, the threshold value is taken as 0.35 m. The confidence level is 0.95, and the corresponding threshold solution is calculated as 0.7076, so the mid-span disturbance value of this studied suspension bridge with 95% guarantee is -0.7076 m. Finally, temperature correction is performed for this threshold, so that the threshold line changes in real time, and the complete dynamic threshold line can be obtained.

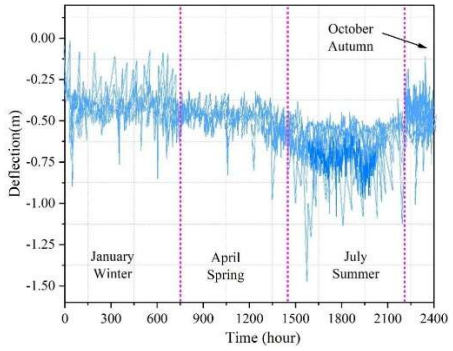

Figure 7: The study of the bridge in the four months of 2024 is the average

IV. Conclusion

In this paper, based on the damage condition strain data of bridge structure, a bridge damage early warning method is developed using LSTM-SSA-BDLM network and integrated learning algorithm under the background of big data and AI-driven, and the conclusions obtained are as follows.

(1)The relationship between temperature and strain can improve the diagnostic accuracy of the anomaly data of LSTM-SSA-BDLM, and the method based on LSTM-SSA-BDLM can well capture and reconstruct the change characteristics of the strain time series.

(2) Using the measured data of the main bridge of Siantang Bridge and the established damage early warning method for condition assessment, the four damage assessment indexes of “k, R^2, b and Ta” are all stably distributed within a certain range, indicating that there is no new damage in the bridge recently.

(3) Considering that with the increase of traffic pressure, more pressure and wear and tear may be formed on related infrastructures such as roads and bridges, this chapter proposes that the threshold values should be updated periodically to accurately reflect the current state and possible risks of the structure, and to avoid serious problems or damages of the structure due to exceeding the capacity by issuing early warning and taking appropriate measures.

References

[1] Zhou, Z., Alcalá, J., & Yepes, V. (2021). Environmental, economic and social impact assessment: Study of bridges in China’s five major economic regions. International journal of environmental research and public health, 18(1), 122.

[2] Zhou, X., & Zhang, X. (2019). Thoughts on the development of bridge technology in China. Engineering, 5(6), 1120-1130.

[3] Luo, T., Xue, X., & Zhang, M. (2024). Exploring sustainable operations management in major infrastructure projects: The case of the Hong Kong-Zhuhai-Macao bridge. Project Management Journal, 55(1), 102-122.
[4] He, X., Wu, T., Zou, Y., Chen, Y. F., Guo, H., & Yu, Z. (2017). Recent developments of high-speed railway bridges in China. Structure and Infrastructure Engineering, 13(12), 1584-1595.
[5] Su, J., Zhang, J., Zhou, J., Hu, C., & Zheng, Y. (2023). Fatigue life assessment of suspenders in tied-arch bridges under random traffic loads and environmental corrosion. International Journal of Civil Engineering, 21(3), 523-540.
[6] Li, Y., Gao, C., Li, C., & Li, Q. (2021). Study on the aging time variation law of mechanical properties of the laminated rubber bearing in coastal bridges considering frictional slip. Shock and Vibration, 2021(1), 3937362.
[7] Ario, I., Yamashita, T., Tsubaki, R., Kawamura, S. I., Uchida, T., Watanabe, G., & Fujiwara, A. (2022). Investigation of bridge collapse phenomena due to heavy rain floods: Structural, hydraulic, and hydrological analysis. Journal of Bridge Engineering, 27(9), 04022073.
[8] Wu, M., Jin, L., & Du, X. (2020). Dynamic responses and reliability analysis of bridge double-column under vehicle collision. Engineering structures, 221, 111035.
[9] Bruno, N., Coïsson, E., Diotri, F., Ferrari, L., Mikolajewska, S., Morra di Cella, U., ... & Zerbi, A. (2019). History, geometry, structure: interdisciplinary analysis of a historical bridge. The International Archives of the Photogrammetry, Remote Sensing and Spatial Information Sciences, 42, 317-323.
[10] Martinelli, P., Galli, A., Barazzetti, L., Colombo, M., Felicetti, R., Previtali, M., ... & di Prisco, M. (2018). Bearing capacity assessment of a 14th century arch bridge in Lecco (Italy). International Journal of Architectural Heritage, 12(2), 237-256.
[11] Bertagnoli, G., Ferrara, M., Miceli, E., Castaldo, P., & Giordano, L. (2024). Safety assessment of an existing bridge deck subject to different damage scenarios through the global safety format ECOV. Engineering Structures, 306, 117859.
[12] Kibria, M. G., Nguyen, K., Villardi, G. P., Zhao, O., Ishizu, K., & Kojima, F. (2018). Big data analytics, machine learning, and artificial intelligence in next-generation wireless networks. IEEE access, 6, 32328-32338.
[13] Zhang, Y., Liu, J., & Shen, W. (2022). A review of ensemble learning algorithms used in remote sensing applications. Applied Sciences, 12(17), 8654.
[14] Comisu, C. C., Taranu, N., Boaca, G., & Scutaru, M. C. (2017). Structural health monitoring system of bridges. Procedia engineering, 199, 2054-2059.
[15] VH, P. K., & Shubhangi, D. C. (2020, July). Design and implementation of real time monitoring of bridge using wireless technology. In 2020 Second International Conference on Inventive Research in Computing Applications (ICIRCA) (pp. 949-953). IEEE.
[16] Lin, T. K., & Chang, Y. S. (2017). Development of a real-time scour monitoring system for bridge safety evaluation. Mechanical Systems and Signal Processing, 82, 503-518.
[17] Qowiy, O. A., Aspar, W. A., Susanto, H., Fiantika, T., Muharam, A., Setiawan, F. D., & Burhanuddin, R. (2024). Online Real-Time Monitoring System of a Structural Steel Railway Bridge Using Wireless Smart Sensors. International Journal on Advanced Science, Engineering & Information Technology, 14(2).
[18] Xu, Y., & Qiu, J. (2023). Internet-based centralized remote real-time long-span bridge health monitoring system. Journal of Computational Methods in Science and Engineering, 23(2), 781-797.
[19] Zhang, G., Zhang, P., Li, X., & Yang, Y. (2024). Dynamic Monitoring of Bridge Structures via an Integrated Cloud and Edge Computing System. International Journal of Advanced Computer Science & Applications, 15(9).
[20] Zeng, K., Li, B., Zeng, S., Zhang, P., & Yang, S. (2025). Real-Time Bridge Deformation Monitoring of Arch Bridge Based on Strain Modal Coordinate Transformation. Journal of Performance of Constructed Facilities, 39(3), 06025001.
[21] Li, S., Wang, W., Lu, B., Du, X., Dong, M., Zhang, T., & Bai, Z. (2023). Long-term structural health monitoring for bridge based on back propagation neural network and long and short-term memory. Structural Health Monitoring, 22(4), 2325-2345.
[22] Kokane, S. R., & Jadhav, P. (2025, January). Real Time Monitoring of Bridge by Using Sensor Technology with Concentration on Deflection Identification. In 2025 1st International Conference on AIML-Applications for Engineering & Technology (ICAET) (pp. 1-5). IEEE.
[23] Riyansyah, M., Wijayanto, P. B., Trilaksono, B. R., Putra, S. A., & Laila, D. S. (2020). Real time bridge dynamic response: Bridge condition assessment and early warning system. Int. J. Adv. Sci. Eng. Inf. Technol., 10(1), 325-330.
[24] Jiang, G., Liang, Q., Wang, H., Ju, Y., Wang, H., Wang, X., ... & Wang, W. (2022). Study on evaluation theory of bridge damage state and methodology on early warning of danger. Advances in Materials Science and Engineering, 2022(1), 6636959.
[25] Zhu, Y. C., Zheng, Y. W., Xiong, W., Li, J. X., Cai, C. S., & Jiang, C. (2024). Online Bridge Structural Condition Assessment Based on the Gaussian Process: A Representative Data Selection and Performance Warning Strategy. Structural Control and Health Monitoring, 2024(1), 5579734.
[26] Wang, Z., Yi, T. H., Yang, D. H., Li, H. N., & Liu, H. (2023). Early Warning of Abnormal Bridge Frequencies Based on a Local Correlation Model under Multiple Environmental Conditions. Journal of Bridge Engineering, 28(2), 04022139.
[27] Li, S., Xin, J., Jiang, Y., Yang, C., Wang, X., & Ran, B. (2024). A novel hybrid model for bridge dynamic early warning using LSTM-EM-GMM. Advances in Bridge Engineering, 5(1), 8.
[28] Priyanshu Sinha,Dinesh Sahu,Shiv Prakash,Tiansheng Yang,Rajkumar Singh Rathore & Vivek Kumar Pandey. (2025). A high performance hybrid LSTM CNN secure architecture for IoT environments using deep learning. Scientific Reports,15(1),9684-9684.
[29] Xiaoqing Wan,Feng Chen,Weizhe Gao,Dongtao Mo & Hui Liu. (2025). Fusion of circulant singular spectrum analysis and multiscale local ternary patterns for effective spectral-spatial feature extraction and small sample hyperspectral image classification.. Scientific reports,15(1),6972.
[30] Jaegyun Park,Dae Won Kim & Jaesung Lee. (2025). HT-AggNet: Hierarchical temporal aggregation network with near-zero-cost layer stacking for human activity recognition. Engineering Applications of Artificial Intelligence,149,110465-110465.